

This discussion paper is/has been under review for the journal Atmospheric Chemistry and Physics (ACP). Please refer to the corresponding final paper in ACP if available.

Spatial variability of aerosol, clouds and rainfall in Himalayas

P. Shrestha and
A. P. Barros

Joint spatial variability of aerosol, clouds and rainfall in the Himalayas from satellite data

P. Shrestha and A. P. Barros

Pratt School of Engineering, Duke University, Durham, NC 27708, USA

Received: 29 January 2010 – Accepted: 1 February 2010 – Published: 12 February 2010

Correspondence to: P. Shrestha (prabhakar.shrestha@duke.edu)

Published by Copernicus Publications on behalf of the European Geosciences Union.

Title Page

Abstract

Introduction

Conclusions

References

Tables

Figures

⏪

⏩

◀

▶

Back

Close

Full Screen / Esc

Printer-friendly Version

Interactive Discussion

Abstract

Satellite-based precipitation, Aerosol Optical Depth (AOD), Cloud Optical Depth (COD), and Aerosol Index (AI) data were used to characterize the linkages among landform and the intra-annual variability of aerosols, cloudiness and rainfall in the Himalayas using Empirical Orthogonal Function (EOF) analysis. The first modes of AOD and AI show the presence of two branches of dust aerosol: over the Indus River basin and the Thar Desert with a sharp west-east gradient parallel to the southern slopes of the Himalayas – the southern Branch; and the second against the slopes of the Tian Shan and over the Takla Makan Desert in the Tibetan Plateau – the northern branch. The second EOF mode of AOD accounts for about 10% of overall variance of AOD. It is attached to the foothills of the Himalayas east of the Aravalli range peaking in April-May followed by a sharp decrease between June and July during the first active phase of the monsoon. The first and second EOF modes of COD and precipitation show consistent patterns against the Central and Eastern Himalayas and along the ocean-land boundaries in western India and the Bay of Bengal. The break in cloudiness and rainfall between the winter and the monsoon seasons is captured well by the second EOF mode of COD and rainfall concurrent with the aerosol build up mode (March-April-May) over the region depicted by the second mode of AOD. The results show that the Aravalli range separates the two different modes of aerosol variability over northern India with dust aerosols to the west and polluted mixed aerosols to the east consistent with its role in regional circulation and precipitations patterns as per Barros et al. (2004) and Chiao and Barros (2006). The region of spatial overlap of the modes of variability of aerosols, clouds and rainfall is captured by the second EOF of MODIS AOD along the southern slopes of the Himalayas east of the Aravalli. It is proposed that this mode maps the area where the indirect radiative effect of aerosols on cloud properties and rainfall is pronounced.

Spatial variability of aerosol, clouds and rainfall in Himalayas

P. Shrestha and
A. P. Barros

Title Page

Abstract

Introduction

Conclusions

References

Tables

Figures

⏪

⏩

◀

▶

Back

Close

Full Screen / Esc

Printer-friendly Version

Interactive Discussion



1 Introduction

Satellite data from various platforms show that the Himalayas act as a barrier that separates a region of abundant aerosols in the Indo-Gangetic Plains (IGP) from the region of pristine air at high altitude in the Tibetan Plateau (Gautam et al., 2009a, Fig. 1a).

5 The accumulation of aerosol in this region can be explained in part by the blocking effect of incoming flows from the Indian subcontinent, but regional-scale circulations modulated by topography also play an important role. Previous studies by Barros et al. (2006), Chiao and Barros (2007), Barros et al. (2004) and Lang and Barros (2002) have shown that the space-time distribution of clouds and rainfall are strongly inter-
10 twined with the terrain in the region. The complex circulation patterns that arise from blocking lead to strong orographic enhancement of precipitation on the southern slopes of the Himalayas.

Lau et al. (2006) used GCM experiments to show that the mixture of black carbon and dust aerosols at higher altitude over the foothills of the Himalaya can act as an elevated heat source in the troposphere, strengthening the monsoon over northern India by intensifying convergence of moist air in the pre-monsoon season. In addition to this mesoscale dynamic effect, Fig. 1b illustrates another possible mechanism of aerosol scavenging by orographic enhancement of clouds and rainfall: aerosols act as condensation nuclei altering cloud drop distributions, and therefore cloud and precipitation
20 microphysical processes, the so called indirect effect. Either via direct and, or indirect radiative forcing and, or via cloud microphysics (Ramanathan et al., 2001), the strong gradient in aerosol concentration appears therefore to be linked to the variability of orographic precipitation along the southern slopes of the Himalayas, thus collocating two of the world's steepest gradients of optical depth and topography in a region critical for
25 the Asian summer monsoon.

Barros et al. (2004) showed that spatial variability of the diurnal cycle of convective activity as depicted by cloudiness in the southern-facing slopes of the Himalayas is strongly tied not only to the overall terrain envelope but also to the west–east

Spatial variability of aerosol, clouds and rainfall in Himalayas

P. Shrestha and
A. P. Barros

Title Page

Abstract

Introduction

Conclusions

References

Tables

Figures



Back

Close

Full Screen / Esc

Printer-friendly Version

Interactive Discussion

Spatial variability of aerosol, clouds and rainfall in HimalayasP. Shrestha and
A. P. Barros

Title Page

Abstract

Introduction

Conclusions

References

Tables

Figures

◀

▶

◀

▶

Back

Close

Full Screen / Esc

Printer-friendly Version

Interactive Discussion

5 succession of ridges and valleys, with the major river valleys that cut through the mountains connecting the Indian sub-continent and the Tibetan Plateau controlling the overall spatial variability of clouds. Liu et al. (2008) could not find evidence of transport between northern India and the Tibetan Plateau across the southern slopes of the Himalayas using CALIPSO data. However, their analysis was limited by the persistent
10 cloud cover during the active phase of monsoon, which precluded detection of plumes associated with low-level flows aligned with major river valleys across the Himalayan range that permit transport from northern India to the Tibetan Plateau (e.g., Barros et al., 2006). In the Central Himalayas, Ramana et al. (2004) reported that the vertical aerosol extinction measured during February 2003 over the Kathmandu Valley showed two local maxima with the secondary maximum at 1.3 km a.g.l. (2.6 km a.s.l.). Both studies, Ramanathan and Ramana (2005) and Ramana et al. (2004), suggest that the primary elevated aerosol layers arises possibly from boundary layer mixing and elevated transport of aerosol from the Indo-Gangetic Plains (IGP), whereas the lower level
15 peak was attributed to local pollution within the Kathmandu Valley (population 2 million). The local aerosol contribution was investigated by Regmi et al. (2003) who argued that boundary layer circulations caused by warm north-westerly flows over cooler shallow south-westerlies (250 m thick) in the Kathmandu Valley could explain the lower level peak. An alternative mechanism was proposed by Hindmann and Upadhyay (2002) who suggested that mountain-valley winds transported Kathmandu Valley pollution to the surrounding hilltops, thus redistributing low level pollutants to higher elevations where they could be picked up by synoptic flows. However, Carrico et al. (2003) found that the surface aerosol signature at Langtang (4000 m altitude, north of Kathmandu Valley) was similar to that associated with long range transport of dust, and they found
20 no evidence of transport from local sources in the Kathmandu Valley. Their measurements of AOD in the Kathmandu Valley (0.37 ± 0.25) in the February-May period, that is the aerosol peak season, are also consistent with Ramana et al. (2004) (AOD in the range of 0.3~0.5). Recently Stone et al. (2009) also reported that carbonaceous aerosol concentrations measured during 2006 at Godavri site in Kathmandu Valley
25

Spatial variability of aerosol, clouds and rainfall in HimalayasP. Shrestha and
A. P. Barros

showed peak concentrations in late March and early April during the dry pre-monsoon season which is consistent with the annually occurring regional haze over the IGP. Further east, Shrestha et al. (2000) measured water soluble aerosols at Phortse (4100 m a.s.l., Himalayan region of Eastern Nepal), which is important from the point of view of aerosol-cloud microphysical interactions. They also report gradual build up of pollutants in the pre-monsoon season (peaking in April-May), which the authors linked to shifts in the large scale circulation, specifically transport from the Indian Gangetic Plains (IGP), and even farther west from the Thar Desert. On the other side, Bonasoni et al. (2008) suggested that the monsoon-driven cleansing mechanism of atmosphere at pollution sources left locally suspended natural particles dominating the AOD at the ABC-Pyramid site (Khumbu Valley, Nepal, 5079 m a.s.l.) during wet season indicating the after-effects of the dominant monsoon season in the region.

One limitation of field studies is the short duration and scattered distribution of surface point measurements that prevent data collection required to extract robust spatial patterns. Nevertheless, all field studies agree on the consistent presence of high concentration of aerosols at high altitude in locations far away from urban sources. Furthermore, the presence of elevated aerosol concentrations of remote origin at high altitudes beyond the edge of rainfall maxima signals the modulation of orographically enhanced precipitation processes upwind, and is consistent with transport from the northern Indian subcontinent to the High Himalaya and the Tibetan Plateau through both deep and shallow flow channels along the N–S oriented river valleys present over the Himalayas (Barros et al., 2004, 2006).

Recently, observations of aerosols and rainfall from multiple satellite platforms have been used to characterize the relationship between aerosols, monsoon rainfall, and monsoon dynamics. Gautam et al. (2009a) present evidence suggesting a close link between pre-monsoon onset tropospheric warming in the IGP and increased atmospheric aerosol loading in the region, which could amplify the land–sea gradient and thus strengthen the initial active phase of the monsoon (June–July). Previously, Gautam et al. (2009b) pointed out that dust outbreaks over the Thar Desert were the critical

Title Page

Abstract

Introduction

Conclusions

References

Tables

Figures

⏪

⏩

◀

▶

Back

Close

Full Screen / Esc

Printer-friendly Version

Interactive Discussion

Spatial variability of aerosol, clouds and rainfall in Himalayas

P. Shrestha and
A. P. Barros

Title Page

Abstract

Introduction

Conclusions

References

Tables

Figures

⏪

⏩

◀

▶

Back

Close

Full Screen / Esc

Printer-friendly Version

Interactive Discussion



source of aerosol loading in the IGP prior to monsoon onset, and therefore interannual variability of the observed tropospheric warming discussed by Gautam et al. (2009a) would be dependent on the frequency and magnitude of dust activity in Northwest India. Bollasina et al. (2008) found that increased aerosol concentrations in May lead to cloud suppression, with increased shortwave radiation reaching and warming the land-surface, thus proposing another pathway to strengthen the land–sea gradient prior to monsoon onset in addition to tropospheric warming. Trend analysis of rainfall during June over an almost twenty-year period showed statistically significant (though modest) increases in monsoon rainfall over regions in the Indian subcontinent that are concurrent with increased aerosol loading in the pre-monsoon period over time (Gautam et al., 2009c). In this manuscript, a concerted analysis of multisensor satellite data is performed to characterize the joint space-time modes of variability of rainfall and aerosol loading in the in the IGP with the objective of mapping the region where local aerosol-cloud-rainfall interactions are dominant vis-à-vis large-scale transport.

For this purpose, we present an assessment of the spatial mode of variability of aerosols and space-time modulation of rainfall using aerosol data products from the Total Ozone Mapping Spectrometer (TOMS) & Moderate Resolution Imaging Spectroradiometer (MODIS), cloud products from MODIS, and rainfall data products from Tropical Rainfall Measuring Mission (TRMM). Section 2 provides an overview of the large scale circulations persistent over the region of study during the identified aerosol build up and decay period. Section 3 describes the remote sensing data used for this study. The EOF analyses of the fields are discussed in Sect. 4, and the joint spatial variability is discussed in Sect. 5. Summary and conclusions are reported in Sect. 6.

2 Regional scale circulation

The Tibetan Plateau and the Himalayas are the dominant topographic features in Asia (Fig. 1a). During the winter season, the westerly jet stream is bifurcated by the Tibetan Plateau, and Shrestha et al. (2000) attributed changes in concentration of pollutants

Spatial variability of aerosol, clouds and rainfall in HimalayasP. Shrestha and
A. P. Barros

in aerosols at high altitude locations in the Himalayas to shifts in the orientation of the southern branch between north-westerly (low concentrations) and south-westerly (high concentrations) orientations. Figure 2a shows the 500 hPa mean horizontal winds and geopotential heights from ERAInterim (reanalysis product from the European Center for Medium Range Weather Forecasts – ECMWF at 1.5 degree resolution, <http://www.ecmwf.int/research/era/do/get/era-interim>) averaged over 10 years from 1998 to 2007 for the months of March, April, May and June. The mean wind profiles suggest that strong westerly wind dominates from March to April and gradually veers north from 18° N to 25° N turning north-westerly over Nepal and northern India. With the onset of Monsoon in June, the southern westerly branch of the jet stream falls apart, causing the main westerly flow to shift northward of to the Tibetan Plateau.

At lower levels, the buildup of the temperature gradient due to the development of a heat low (deepest in July) over the arid regions of Pakistan and North-West India during May pulls low level westerly flow from the Arabian Sea and the Somali low-level jet (Findlater, 1969; Wu et al., 1999). Figure 2b shows the 900 hPa horizontal wind and geopotential height from the ERAInterim, averaged over 10 years from 1998 to 2007 for the months of March, April, May and June. North-westerly flow is prevalent in March along the IGP. Note the two circulation patterns west and east of the Western and Eastern Ghat Mountains on the west and east coasts of the Indian subcontinent, respectively that persist through April, as well as the strong low-level jet at 20~25° N crossing over the Thar Desert into the IGP. The mean wind flow over the IGP weakens in the following months, whereas the westerlies further south strengthen and veer northeastward along the Eastern Ghats, and a weak convergence zone forms over the IGP below the Nepal-India border. Meanwhile, on the northwestern sector of the Indian subcontinent, northerly flow along the western border of Afghanistan becomes stronger in June, mixes with the westerly flow from the Arabian Sea, and veers northward along the India-Pakistan border. Strong westerly flow is well established in the lower-half of the Indian subcontinent up to the Bay of Bengal. This westerly flow bifurcates at the Aravalli range turning south-westerly over the Thar Desert, whereas it

Title Page

Abstract

Introduction

Conclusions

References

Tables

Figures

⏪

⏩

◀

▶

Back

Close

Full Screen / Esc

Printer-friendly Version

Interactive Discussion

remains westerly, south of the Aravalli range. Dust storms in the IGP during the pre-monsoon season have been associated with dusts lifted mainly from the Thar Desert and arid regions farther west along the path of the westerlies (Gautam et al., 2007). The observed blocking and convergence effects over the Indus River basin and along the foothills of the Himalayas over Nepal create favourable conditions for the accumulation of both remote and local aerosol establishing sharp regional gradients.

3 Satellite data

Table 1 describes the various satellite datasets used for the study. Observations from the Moderate Resolution Imaging Spectroradiometer (MODIS) instrument aboard the Terra and Aqua satellites are used to study the variability of aerosol optical depth (AOD) over the region. The MODIS aerosol retrieval is more accurate where albedo is low over land (dark vegetation, Kaufman et al., 1997; Hsu et al., 2004). The algorithm over land is applied to 10 km × 10 km areas to minimize the signal noise ratio (SNR) to obtain the Level 1 products. Here, we used Level 3 daily data products at monthly time-scales sorted into an 1° × 1° equal angle grid. The missing values in MODIS AOD data over bright reflecting surfaces were filled with the concurrent spatial mean of the AOD for this analysis.

The aerosol index (AI) data from Total Ozone Mapping Spectrometer (TOMS) instrument was also used for the study:

$$AI = 100 \log_{10} \left(\frac{I_{\text{Meas.360}}}{I_{\text{Calc.360}}} \right) \quad (1)$$

where $I_{\text{Meas.360}}$ is the measured 360 nm radiance, and $I_{\text{Calc.360}}$ is the calculated 360 nm radiance assuming a Rayleigh atmosphere. The low value of near-UV albedo for land/water bodies combined with the large molecular scattering in this region of the spectrum allows for a robust determination of aerosol properties by TOMS. However, the retrieved quantities are sensitive to the height of UV-absorbing aerosol layer over

Spatial variability of aerosol, clouds and rainfall in Himalayas

P. Shrestha and
A. P. Barros

Title Page

Abstract

Introduction

Conclusions

References

Tables

Figures

⏪

⏩

◀

▶

Back

Close

Full Screen / Esc

Printer-friendly Version

Interactive Discussion



Spatial variability of aerosol, clouds and rainfall in Himalayas

P. Shrestha and
A. P. Barros

Title Page

Abstract

Introduction

Conclusions

References

Tables

Figures

⏪

⏩

◀

▶

Back

Close

Full Screen / Esc

Printer-friendly Version

Interactive Discussion

the ground, but are not sensitive to the presence of non-absorbing aerosol, as well as smoke in the lowest 1 km of the atmosphere except for colored aerosols like mineral dust (Torres et al., 2002). Further, it is not possible to distinguish among different UV-absorbing aerosol types leading to AI errors if the aerosol types for different geographical regions are misclassified (see <http://toms.gsfc.nasa.gov/news>). Although the TOMS data from Earth Probe are available between 1996 and 2005, the time-window for this study was constrained to the period 1998 to 2005 for subsequent comparison against TRMM rainfall data which are available from 1998 onward.

Precipitation estimates were obtained from the TRMM 3B-43 data product (<http://daac.gsfc.nasa.gov/data/datapool/TRMM/>), which are derived from the combination of 3-h merged high-quality/IR estimates with the monthly accumulated Climate Assessment and Monitoring System (CAM5) or Global Precipitation Climatology Centre (GPCP) rain gauge analysis (Huffmann et al., 2007). Monthly precipitation estimates gridded on $0.25^\circ \times 0.25^\circ$ global grids are available since 1998.

Finally, MODIS Level 3 cloud optical depth (COD) was used to study the spatial and temporal modes of variability in cloudiness. The retrieval of cloud optical depth requires information about particle phase and cloud cover, and a radiative transfer model is used for the inversion algorithm. The retrieval is valid for single-layer, liquid water clouds, plane-parallel geometry, and errors might arise for multiple layer clouds and when ice is present (King et al., 1998). Missing values (small number) in MODIS COD were filled by linear interpolation in time. Similar to the MODIS Level 3 aerosol products, the Level 3 cloud optical depth also contains the statistics derived from Level 2 products gridded at $1^\circ \times 1^\circ$ spatial resolution (see King et al., 1998 for more details).

4 EOF analysis

EOF analysis when applied to a space-time dataset can be used to decompose the observed variability into a set of orthogonal spatial patterns (EOFs), which are invariant in time, and a set of time series, the expansion coefficients (ECs), which are invariant

in space (e.g., North et al., 1982; Behera et al., 2003; Perry and Neimann, 2007; Giovanntone and Barros, 2008; among many others). In this study, we conducted EOF analysis using the covariance method (von Storch and Zwiers, 1999) to study temporal and spatial anomalies of rainfall, aerosols and cloudiness over a larger spatial domain covering the IGP in the south to the Tibetan Plateau in the North.

4.1 Aerosol variability

The first EOF mode (EOF 1) from MODIS and TOMS explain 58% and 53% of the overall AOD and AI field variances, respectively (see Figs. 3 and 4). Both modes show the presence of two branches of the dust aerosol distribution: the southern branch (SB) over the Indus River basin and Thar Desert with a sharp west–east gradient parallel to the southern slopes of the Himalayas; and the northern branch against the slopes of the Tian Shan and over the Takla Makan Desert in the Tibetan Plateau. The northern branch is associated with the active dust storms in the Takla Makan Desert in the Xinjiang region of Western China (Figs. 1b and 5a). A sandy haze covers most of the oval shaped desert, which sits in a depression between two high mountain ranges: the Tian Shan to the north, and the Kunlun to the south. Earlier, Lau et al. (2006) and Lau and Kim (2006) noted that the two branches of AOD should be composed primarily of dust aerosols originating from the deserts, whereas carbonaceous aerosols from biomass burning over the northwestern India and Pakistan should be present in the chemical composition of the southern branch. Analysis of 900 hPa ERAInterim wind fields (Fig. 2b) indicates that the blocking of the westerly winds by the mountain ranges in the north and west of Indus River basin is primarily responsible for the buildup of southern branch. This blocking creates a favorable spot for aerosol accumulation, which is sustained by the dust originating from the Thar Desert from and arid regions in Pakistan, Afghanistan and farther west. Figure 5b shows the MODIS visible image of a storm that stretches for over 1000 km (about 620 miles) from Central Pakistan into Northern India in June 2005, which exhibits morphology typical of dust storms in the region in spring and summer. The heat low over the desert results in strong

Spatial variability of aerosol, clouds and rainfall in Himalayas

P. Shrestha and
A. P. Barros

Title Page

Abstract

Introduction

Conclusions

References

Tables

Figures



Back

Close

Full Screen / Esc

Printer-friendly Version

Interactive Discussion



Spatial variability of aerosol, clouds and rainfall in HimalayasP. Shrestha and
A. P. Barros[Title Page](#)[Abstract](#)[Introduction](#)[Conclusions](#)[References](#)[Tables](#)[Figures](#)[⏪](#)[⏩](#)[◀](#)[▶](#)[Back](#)[Close](#)[Full Screen / Esc](#)[Printer-friendly Version](#)[Interactive Discussion](#)

convergence inducing dry convection that carries surface dust aloft to be subsequently transported away by the prevailing winds (see the dust plume in Fig. 5b). The blocking effect of the terrain is evident from the sharp W–E gradient of aerosol concentration along the foothills of the Himalayas in the southern branch (SB) of EOF1 for TOMS AI and MODIS AOD (68° E to 80° E). The MODIS SB EC1 indicates that AOD starts building up in April-May, peaks in July, and is followed by a decline in August and September consistent with the retreat of the monsoon. Persistent build up of aerosol in May-June-July is present over the six year span of the study (2002–2007). This aerosol build up and the decline in the second-half of the monsoon is explained by the strengthening and decay phases of the low level westerly flow that can bring pollutants all the way from the east coast of Africa and the Middle East (Lau et al., 2006).

The second EOF mode (EOF2) of MODIS AOD, bounded by the Aravalli range in the west and by the Bay of Bengal in the east, accounts for 10% of the overall AOD variance. Earlier studies by Chiao and Barros (2007) focused on the role of the Aravalli range as a hydro-meteorological dryline separating western, drier and more unstable air masses from moist and relatively stable air masses from the Bay of Bengal. Likewise, note the well defined belt of haze on the foothills of the Himalayas eastward of 80° E in the north-eastern sector of the IGP (see Fig. 6). This also explains the phase shift in the build-up and decay of the EOF2 of MODIS AOD (March-April, peaking in April or May) with regard to EOF1. The development of low level convergence in this zone during the month of May as observed in the 900 hPa wind fields (Fig. 2b) results in the accumulation of emissions from the IGP that mix with pollutants from the west (especially dust) and the east, creating a more mixed aerosol loading. The decline of the second EOF mode in June is due to the onset of the monsoon in northern India and contrasts with the August-September decline of the first EOF mode. Thus, the Aravalli range appears to separate two different modes of regional aerosol variability in the lower atmosphere.

4.2 Rainfall and cloud variability

Strong gradients of cloudiness and rainfall are aligned along the Western Ghats in the SW of India, the SW coastlines of Bangladesh and Burma, and the southern slopes of the Himalayas. The modes of rainfall and cloudiness are highly correlated indicating clouds as tracers of the anomalous monsoon rainfall. The first EOF mode (EOF 1) of TRMM 3B-43 rainfall (Fig. 7) explains 63% of the overall variance and captures the strong gradient of monsoon rainfall prevalent over the Western Ghats and near the Bay of Bengal, as well as a substantial amount of rainfall in Central India. The scarcity of monsoon rainfall over the arid region of NW India is concurrent with the strong gradient of aerosol build-up in the region which peaks in July as per the first EOF mode of MODIS AOD and TOMS AI. As discussed before, the convective activity is confined to the east of the Aravalli range during the monsoon. The first EOF mode of rainfall displays a strong gradient aligned with the lower foothills of the Himalayas during the JJAS period consistent with the orographic modulation of low level depressions that propagate westward from the Bay of Bengal and produce large rainfall (Lang and Barros, 2002). Although the EOF analysis of monthly TRMM3B-43 rainfall data used here is not able to discern the active and break phases of monsoon that take place at sub-monthly time-scales (Krishnamurthy and Shukla, 2000; Barros et al., 2004), the presence of large spatial patterns of the same sign in northern India and the southern foothills of the Himalaya indicates that the dominant mode of the JJAS seasonal variation of rainfall is robust.

The first EOF mode (EOF1) of the MODIS Cloud Optical Depth (COD, Fig. 8) explains 35% of the variance and shows cloudiness associated with the monsoon over the Western Ghats of southwest India and the SW coastlines of Bangladesh and Burma. Variation over the southern slopes of the Himalayas is only apparent in the second mode (EOF2) of MODIS COD corresponding to 12% of the variance consistent with the highly transient nature of regional circulation in the region. The EOF2 pattern is linked to westerly disturbances propagating eastward along the foothills of Himalayas

Spatial variability of aerosol, clouds and rainfall in Himalayas

P. Shrestha and
A. P. Barros

Title Page

Abstract

Introduction

Conclusions

References

Tables

Figures

⏪

⏩

◀

▶

Back

Close

Full Screen / Esc

Printer-friendly Version

Interactive Discussion

Spatial variability of aerosol, clouds and rainfall in HimalayasP. Shrestha and
A. P. Barros

Title Page

Abstract

Introduction

Conclusions

References

Tables

Figures

⏪

⏩

◀

▶

Back

Close

Full Screen / Esc

Printer-friendly Version

Interactive Discussion

during the winter and the dominant monsoon season (JJAS). Interestingly, the break in cloudiness during the dry period between the winter and the monsoon seasons in the second mode of MODIS COD (EC2) is concurrent with the regional aerosol build-up phase (March-April-May) in the pre-monsoon season seen in MODIS AOD (EC2).

5 EOF2 also shows distinct cloudiness patterns in the Northern India Convergence Zone (NICZ, Barros et al., 2004) around May and then later in October–November. The May cloudiness pattern precedes the onset of the summer monsoon as cloud systems propagate northward. In the fall (October–November), the cloudiness pattern is consistent with post-monsoon conditions (clear skies, low rainfall).

10 These processes are captured well by examining the temporal correlation of the ECs between TRMM rainfall and MODIS COD and AOD. The highest correlation ($r\sim 0.7$) is found among the first modes of MODIS AOD, COD and TRMM precipitation at zero lag and a correlation length of six-months. This expresses the fact that the same large-scale dynamics are governing aerosol and moisture transport in the region. Nearly as high correlation values were found between the EC2 of AOD and the EC1 of TRMM rainfall though they take place with a lag of three months with AOD leading rainfall. Similarly, high correlations were obtained for the correlation between EC2 of AOD and EC1 of COD ($r\sim 0.65$, lag=3 months), thus expressing the relationship between cloud optical depth and precipitation mediated by cloud processes and illustrates how the

20 aerosol buildup in March-April-May is cut off by the monsoon onset in June. The correlation between EC2 of MODIS AOD and EC2 of TRMM rainfall and MODIS COD switches from negative at lag zero to a positive peak at three months ($r\sim 0.3$ for rainfall and $r\sim 0.4$ for COD) and a second positive maximum ($r\sim 0.35$ for rainfall and $r\sim 0.4$ for COD) at 9–10 months lag consistent with monsoon activity patterns. The three-month lag is associated with the peaks in rainfall and cloudiness during the monsoon season,

25 whereas the 10-month lag is associated with peaks in cloudiness and rainfall in the pre-monsoon season suggesting cloud-aerosol interactions. In the fall (6-month lag), the correlation reaches its lowest value ($r\sim -0.6$) consistent with post-monsoon conditions discussed above.

5 Joint variability

The coupled modes of variability between the time series of two fields were analyzed by singular value decomposition (SVD) of the covariance matrix between the two fields. The relevant property of the left and right singular vectors obtained from SVD is that they maximize covariance and hence are the patterns themselves. The expansion coefficients (a, b) are obtained as the projection of the fields on the left and right singular vectors, respectively (see Bretherton et al., 1992; von Storch and Zwiers, 1999 for detailed discussions). The analysis was applied to pairs of TRMM precipitation, MODIS AOD and COD, aggregated at spatial resolution of 1×1 degree, for a time span of six years from 2000 to 2006. Further, to identify any causal relationships among the fields, cross-correlation was applied to the expansions coefficients of the pair of patterns (f_x, f_y) at different lags (Table 2). All the patterns exhibited a strong correlation at zero lag.

5.1 TRMM precipitation-MODIS AOD

The first pair of patterns has a maximum squared cross-covariance of 96.32% and resembles the first EOF modes associated with each field (Fig. 9). The main features of the TRMM precipitation are the heavy rainfall over the Western Ghats of India, Bay of Bengal, and a narrow strip of precipitation along the Himalayas, associated with the strong monsoon season. The MODIS AOD shows a dominant mode in the Indus valley with sharp W–E gradient running parallel to the southern slopes of Himalayas. The patterns and the lag coefficients are consistent with the timing and spatial signature of monsoon dynamics. The expansion coefficients of the first pair of pattern show a strong correlation at zero lag over the monsoon season (Fig. 10a). The second pair of patterns has a squared cross-covariance of 2.68% and resembles the second EOF modes associated with each field. Notice in particular the MODIS AOD pattern extending from $80^\circ \text{E} \sim 90^\circ \text{E}$ which peaks during the non-monsoon season but is “washed away” by the rain during the monsoon season (Fig. 9). The pattern shows a collocated region of anomalous aerosol and precipitation, where aerosol rain interaction takes place.

Spatial variability of aerosol, clouds and rainfall in Himalayas

P. Shrestha and
A. P. Barros

Title Page

Abstract

Introduction

Conclusions

References

Tables

Figures

⏪

⏩

◀

▶

Back

Close

Full Screen / Esc

Printer-friendly Version

Interactive Discussion

5.2 MODIS COD and AOD

Similar to the results obtained for TRMM Precipitation and MODIS AOD, the first pair of covariance patterns for MODIS COD and AOD has the maximum squared covariance of 89.5% , and the MODIS AOD pattern resembles its first mode (Fig. 11). The cloudiness in the first pattern however differs from the first mode of MODIS COD, with a strong signal in the Bay of Bengal. It is only in the second pattern that the distinct monsoon signal with cloudiness over the Western Ghats and Bay of Bengal and Eastern Ghats becomes distinctively apparent and is coupled with the built up of aerosol optical depth over the Arabian Sea. The expansion coefficient of the MODIS COD for the second pair of pattern explains the cloudiness during the monsoon season over the Western and Eastern Ghats of India during the summer monsoon and the cloudiness over the Himalayas, North-Eastern India and over the north-western analysis domain during the remainder of the year (Fig. 10b). Similar to the second pair of TRMM precipitation and MODIS AOD, an inverted L-shaped pattern of aerosol is visible along the north-eastern part of India bounded by the Himalayas over Nepal. This aerosol pattern is present during the non-monsoon season and correlates with the cloudiness pattern along the Himalayas and North-Eastern India as well as the distinct cloudiness pattern for the north-western analysis domain related to westerly disturbances.

6 Summary

The objective of this study is to identify the domain of joint space-time variability of landform, aerosols, clouds and rainfall along the south facing slopes of the Himalayas. The space-time patterns of the first EOF modes of satellite-based precipitation (TRMM 3B-43), Aerosol Optical Depth (AOD), Cloud Optical Depth (COD), Aerosol Index (AI), and Cloud Optical Depth (COD) reflect large-scale circulation patterns modulated by the Himalayan range. Indeed, the overall EOF spectra (Fig. 12) are consistent with the results pointed out by Barros et al. (2004) for the Himalayas and by Giovannetone and

Spatial variability of aerosol, clouds and rainfall in Himalayas

P. Shrestha and
A. P. Barros

Title Page

Abstract

Introduction

Conclusions

References

Tables

Figures



Back

Close

Full Screen / Esc

Printer-friendly Version

Interactive Discussion

Barros (2009) for the Andes with the first EOF mode explaining 45–55% of the overall variance of all observations in continental regions where orography plays the dominant role in organizing regional circulation and transport patterns.

Analysis of the regional mean flow shows that the blocking and convergence effects over the Indus River basin and Thar Desert and along the foothills of the Himalayas over Nepal create favourable conditions for the accumulation of both remote and local aerosol establishing sharp regional gradients, which is consistent with the spatial modes of aerosol variability obtained from EOF analysis. Two different modes of aerosol buildup that develop east and west of the Aravalli range can be clearly identified from the analysis of the space-time patterns defined by EOFs and ECs. The spatial pattern of the second mode of AOD is collocated with the first and second mode of TRMM precipitation and MODIS COD, respectively. The first EOF modes of COD and precipitation show consistent patterns against the Central and Eastern Himalayas and the Western Ghats and along the ocean–land boundaries in Western India and the Bay of Bengal. The break in cloudiness between the winter and the monsoon captured by the second EC of MODIS COD coincides with the aerosol build up mode (March–April–May) over the region corresponding to the transition between distinct modes of cloudiness from cold (winter) to warm (monsoon) seasons. These results confirm previous work regarding the relationship between the anomalous aerosol buildup during the months of March, April and May and the pre-monsoon rainfall regime by aerosol cloud interaction. Finally, this study identifies the spatial pattern of the EOF2 of MODIS AOD east of the Aravalli range as a region of pronounced aerosol-cloud-rainfall interactions.

Acknowledgement. This research was funded in part by NASA Earth System Science Fellowship with the first author and by NASA grants NNX07AK40G at Duke University. The data for this study was obtained from the Giovanni online data system, developed and maintained by the NASA Goddard Earth Sciences (GES) Data and Information Services Center (DISC).

Spatial variability of aerosol, clouds and rainfall in Himalayas

P. Shrestha and
A. P. Barros

Title Page

Abstract

Introduction

Conclusions

References

Tables

Figures

⏪

⏩

◀

▶

Back

Close

Full Screen / Esc

Printer-friendly Version

Interactive Discussion

References

- Barros, A. P., Kim, G., Williams, E., and Nesbitt, S. W.: Probing orographic controls in the Himalayas during the monsoon using satellite imagery, *Nat. Hazards Earth Syst. Sci.*, 4, 29–51, 2004,
5 <http://www.nat-hazards-earth-syst-sci.net/4/29/2004/>.
- Barros, A. P., Chiao, S., Lang, T., Burbank, D., and Putkonen, J.: From weather to climate – seasonal and interannual variability of storms and implications for erosion processes in the Himalaya, *Geol. S. Am. S.*, 398, 17–38, 2006.
- Behera, S., Rao, S., Saji, H., and Yamagata, T.: Comments in “A cautionary note on the interpretation of EOFs”, *J. Climate*, 16, 1087–1093, 2003.
- 10 Bonasoni, P., Laj, P., Angelini, F., Arduini, J., Bonafe, U., Calzolari, F., Cristofanelli, P., Decesari, S., Facchini, M. C., Fuzzi, S., Gobbi, G. P., Maione, M., Marinoni, A., Petzold, A., Roccato, F., Roger, J. C., Sellegri, K., Sprenger, M., Venzac, H., Verza, G. P., Villani, P., and Vuillermoz, E.: The ABC-Pyramid Atmospheric Research Observatory in Himalaya for aerosol, ozone and halocarbon measurements, *Sci. Total Environ.*, 391, 252–261, 2008.
- 15 Bretherton, C. S., Smith, C., and Wallace, J. M.: An intercomparison of methods for finding coupled patterns in climate data, *J. Climate*, 5, 541–559, 1992.
- Bollasina, M. and Nigam, S.: Absorbing aerosols and summer monsoon evolution over South Asia: an observational portrayal, *J. Climate*, 21, 3221–3239, 2008.
- 20 Carrico, C. M., Bergin, M. H., Shrestha, A. B., Dibb, J. E., Gomes, L., and Harris, J. M.: The importance of carbon and mineral dust to seasonal aerosol properties in the Nepal Himalaya, *Atmos. Environ.*, 37, 2811–2824, 2003.
- Chiao, S. and Barros, A. P.: A numerical study of hydrometeorological dryline in Northwest India during the monsoon, *J. Meteorol. Soc. Jpn.*, 85A, 337–361, 2007.
- 25 Findlater, J.: A major low-level air current near the Indian Ocean during the northern summer, *Q. J. Roy. Meteor. Soc.*, 95(404), 362–380, 1963.
- Gautam, R., Hsu, N. C., Kafatos, M., and Tsay, S.-C.: Influences of winter haze on fog/low cloud over the Indo-Gangetic plains, *J. Geophys. Res.*, 112, D05207, doi:10.1029/2005JD007036, 2007.
- 30 Gautam, R., Hsu, N. C., Lau, K. M., Tsay, S. C., and Kafatos, M.: Enhanced pre-monsoon warming over the Himalayan-Gangetic region from 1979–2007, *Geophys. Res. Lett.*, 36, L07704, doi:10.1029/2009GL037641, 2009a.

Spatial variability of aerosol, clouds and rainfall in Himalayas

P. Shrestha and
A. P. Barros

Title Page

Abstract

Introduction

Conclusions

References

Tables

Figures

⏪

⏩

◀

▶

Back

Close

Full Screen / Esc

Printer-friendly Version

Interactive Discussion

Gautam, R., Liu, Z., Singh, R. P., and Hsu, C. N.: Two contrasting dust-dominant periods over India observed from MODIS and CALIPSO data, *Geophys. Res. Lett.*, 36, L06813, doi:10.1029/2009GL036967, 2009b.

Gautam, R., Hsu, N. C., Lau, K.-M., and Kafatos, M.: Aerosol and rainfall variability over the Indian monsoon region: distributions, trends and coupling, *Ann. Geophys.*, 27, 3691–3703, 2009,
http://www.ann-geophys.net/27/3691/2009/.

Giovannetone, J. P. and Barros, A. P.: A remote sensing survey of the role of landform on the organization of orographic precipitation in Central and Southern Mexico, *J. Hydrometeorol.*, 9, 1267–1283, 2008.

Hindman, E. E. and Upadhyay, B. P.: Air pollution transport in the Himalayas of Nepal and Tibet during the 1995–1996 dry season, *Atmos. Environ.*, 36, 727–739, 2002.

Huffman, G. J., Adler, R. F., Curtis, S., Bolvin, D. T., and Nelkin, E. J.: Global rainfall analysis at monthly and 3-h time scales, *Adv. Glob. Change Res.*, 28, 291–305, 2007.

Hsu, N. C., Tsay, S. C., King, M. D., and Herman, J. R.: Aerosol properties over bright-reflecting source regions, *IEEE T. Geosci. Remote*, 42, 557–569, 2004.

Kaufman, Y. J., Tanre, D., Remer, L. A., Vermote, E. F., Chu, A., and Holben, B. N.: Operational remote sensing of tropospheric aerosol over land from EOS moderate resolution imaging spectroradiometer, *J. Geophys. Res.*, 102(D14), 17051–17067, 1997.

King, M. D., Tsay, S.-C., Platnick, S. E., Wang, M., and Liou, K.-N.: Cloud Retrieval Algorithms for MODIS: Optical Thickness, Effective Particle Radius, and Thermodynamic Phase, Products: 06_L2, 08_D3, 08_E3, 08_M3, ATBD Reference Number: ATBD-MOD-05, 1998.

Krishnamurthy, V. and Shukla, J.: Intraseasonal and interannual variability of rainfall over India, *J. Climate*, 13, 4366–4377, 2000.

Lang, T. J. and Barros, A. P.: An investigation of the onsets of 1999 and 2000 monsoons in Central Nepal, *Mon. Weather Rev.*, 130, 1299–1316, 2002.

Lau, K.-M. and Kim, K.-M.: Observational relationship between aerosol and Asian monsoon rainfall, and circulation, *Geophys. Res. Lett.*, 33, L21810, doi:10.1029/2006GL027546, 2006.

Lau, K. M., Kim, M. K., and Kim, K. M.: Asian summer monsoon anomalies induced by aerosol direct forcing: the role of the Tibetan Plateau, *Clim. Dynam.*, 26, 855–864, 2006.

Perry, A. M. and Neimann, J. D.: Analysis and estimation of soil moisture at catchment scale using EOFs, *J. Hydrol.*, 334, 388–404, 2007.

Spatial variability of aerosol, clouds and rainfall in Himalayas

P. Shrestha and
A. P. Barros

Title Page

Abstract

Introduction

Conclusions

References

Tables

Figures

◀

▶

◀

▶

Back

Close

Full Screen / Esc

Printer-friendly Version

Interactive Discussion

Spatial variability of aerosol, clouds and rainfall in HimalayasP. Shrestha and
A. P. Barros[Title Page](#)[Abstract](#)[Introduction](#)[Conclusions](#)[References](#)[Tables](#)[Figures](#)[⏪](#)[⏩](#)[◀](#)[▶](#)[Back](#)[Close](#)[Full Screen / Esc](#)[Printer-friendly Version](#)[Interactive Discussion](#)

Spatial variability of aerosol, clouds and rainfall in Himalayas

P. Shrestha and
A. P. Barros

Table 1. List of data products used from different satellite platforms.

Sino.	Description	Satellite	Coverage
1	Gridded daily aerosol index (AI)	Earth Probe TOMS	Jan 98~Dec 05
2	Gridded monthly AOD	Terra MODIS	Jan 02~Dec 07
3	Gridded monthly COD	Terra MODIS	Jan 02~Dec 07
4	Gridded monthly accumulated rainfall	TRMM 3B43 (V6)	Jan 98~Dec 07

[Title Page](#)
[Abstract](#)
[Introduction](#)
[Conclusions](#)
[References](#)
[Tables](#)
[Figures](#)
[Back](#)
[Close](#)
[Full Screen / Esc](#)
[Printer-friendly Version](#)
[Interactive Discussion](#)

Spatial variability of aerosol, clouds and rainfall in Himalayas

P. Shrestha and
A. P. Barros

Table 2. Cross-correlation between the expansion coefficients of the pair of patterns.

TRMM precipitation-MODIS AOD								
Lag	-3	-2	-1	0	1	2	3	Covariance explained
	-0.036	0.43	0.77	0.89	0.68	0.30	-0.14	96.32% ($a1,b1$)
	-0.54	-0.26	0.34	0.79	0.47	0.1	-0.2	2.68% ($a2,b2$)
MODIS COD and MODIS AOD								
Lag	-3	-2	-1	0	1	2	3	Covariance explained
	-0.125	0.117	0.23	0.55	0.44	0.25	0.11	89.48% ($a1,b1$)
	-0.168	0.269	0.64	0.84	0.69	0.41	0.04	8.74% ($a2,b2$)

Title Page

Abstract

Introduction

Conclusions

References

Tables

Figures

⏪

⏩

◀

▶

Back

Close

Full Screen / Esc

Printer-friendly Version

Interactive Discussion

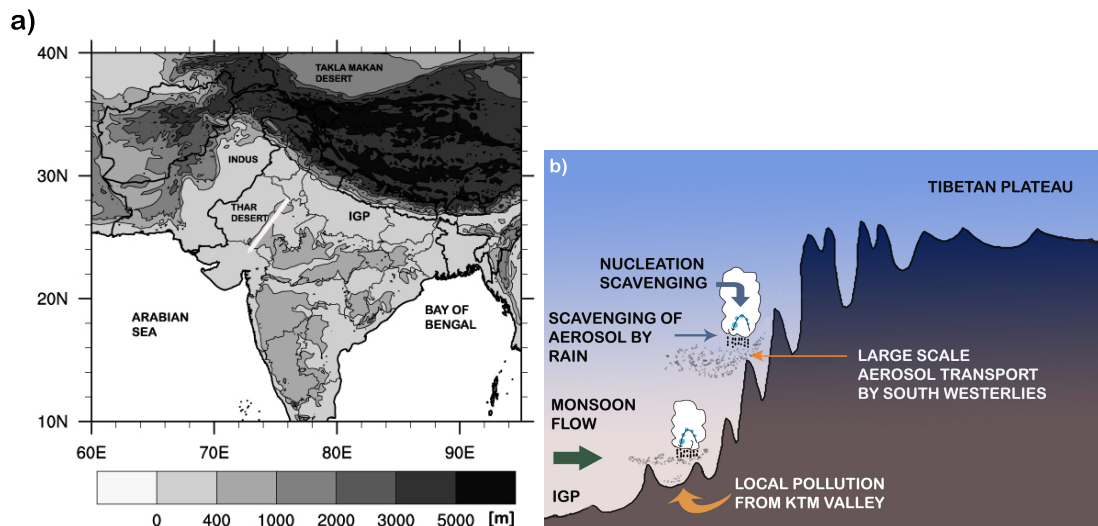


Fig. 1. (a) The Tibetan Plateau and the Himalayas are unique features of Asia with the Indian Gangetic Plain (IGP) and Indus River basin on the southern slopes and Takla Makan Desert on the northern slopes of the Tibetan Plateau. Thar Desert lies on the western slopes of the Aravalli range (straight white strip). Elevation contours are plotted at 400, 1000, 2000, 3000 and 5000 m. Topography was obtained from the USGS gtopo30 data. **(b)** Processing of aerosols by clouds along the North–South cross-section passing through Kathmandu Valley in Central Nepal.

Spatial variability of aerosol, clouds and rainfall in Himalayas

P. Shrestha and
A. P. Barros

Title Page

Abstract

Introduction

Conclusions

References

Tables

Figures

◀

▶

◀

▶

Back

Close

Full Screen / Esc

Printer-friendly Version

Interactive Discussion

Spatial variability of aerosol, clouds and rainfall in Himalayas

P. Shrestha and
A. P. Barros

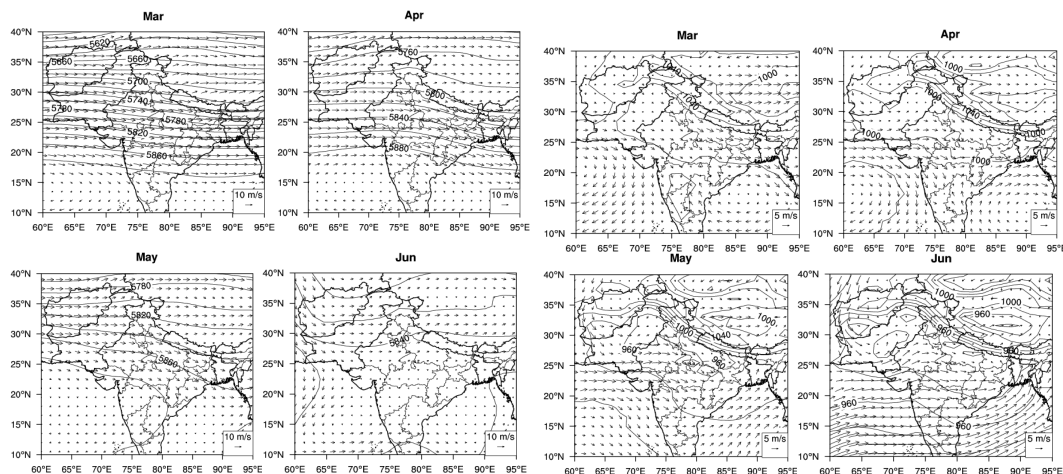


Fig. 2. (a) Mean geopotential height (m) and horizontal wind (m/s) at 500 hPa from 1998 to 2007 for the month of March, April, May and June. ERAInterim (<http://www.ecmwf.int/research/era/do/get/era-interim>) dataset were used for the above analysis. (b) Mean geopotential height (m) and horizontal wind (m/s) at 900 hPa from 1998 to 2007 for the month of March, April, May and June. ERAInterim (<http://www.ecmwf.int/research/era/do/get/era-interim>) dataset were used for the above analysis.

Title Page

Abstract

Introduction

Conclusions

References

Tables

Figures

◀

▶

◀

▶

Back

Close

Full Screen / Esc

Printer-friendly Version

Interactive Discussion

Spatial variability of aerosol, clouds and rainfall in Himalayas

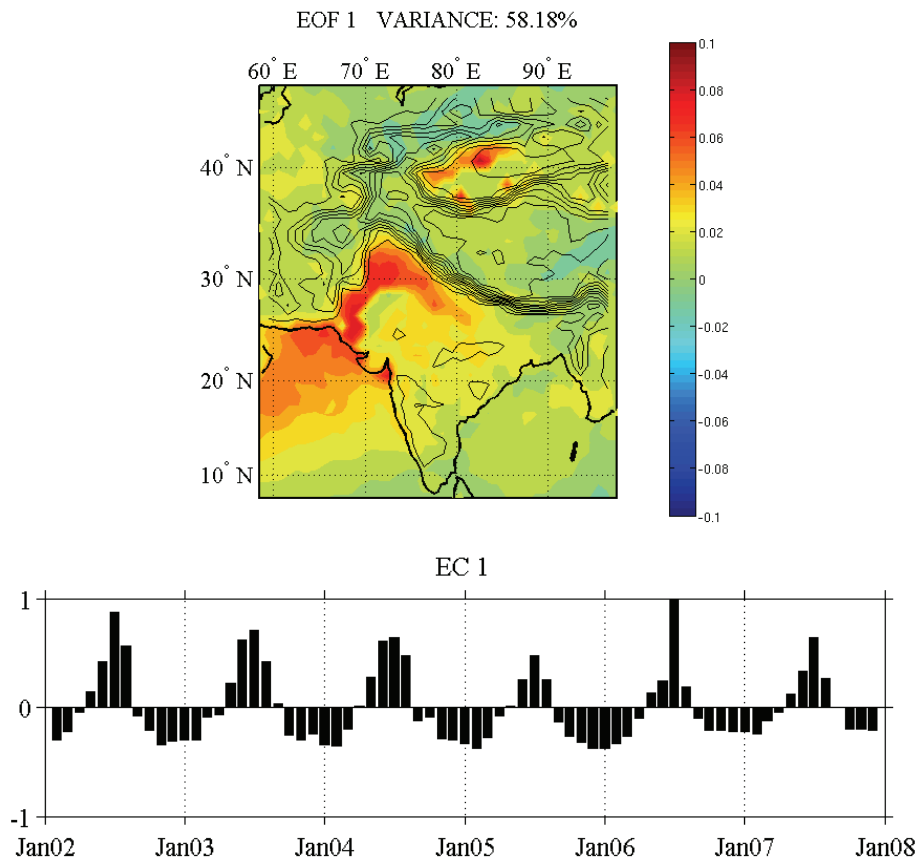
P. Shrestha and
A. P. Barros

Fig. 3. EOF 1 and EC1 computed from MODIS monthly aerosol optical depth (AOD). [The gridded products in MODIS uses QC (Quality Assurance Confidence) flags for weighting the 10 km product, giving higher weightings for retrieval with QAC=3 and not using retrievals with QAC=0.] Terrain contours are plotted at 500 m interval from 500 m to 8000 m.

[Title Page](#)[Abstract](#)[Introduction](#)[Conclusions](#)[References](#)[Tables](#)[Figures](#)[◀](#)[▶](#)[◀](#)[▶](#)[Back](#)[Close](#)[Full Screen / Esc](#)[Printer-friendly Version](#)[Interactive Discussion](#)

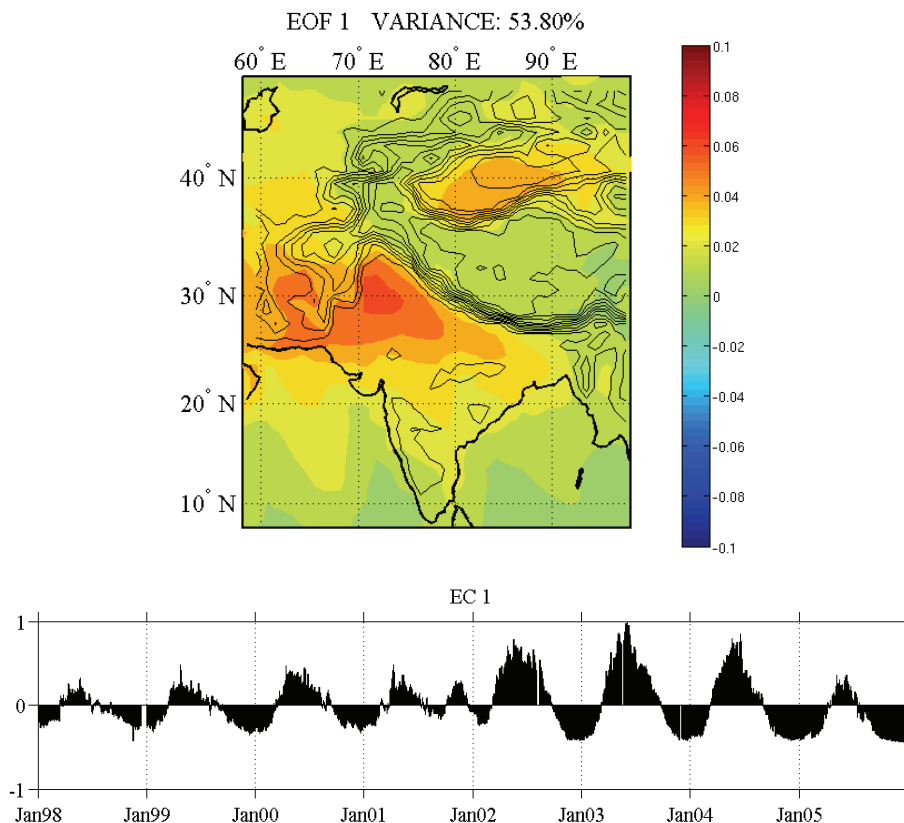
Spatial variability of aerosol, clouds and rainfall in HimalayasP. Shrestha and
A. P. Barros

Fig. 4. EOF 1 and EC1 computed from TOMS daily aerosol index (AI) indicate a dominant mode over the Indus River basin and Thar Desert with a sharp west–east gradient along the southern slopes of the Himalayas.

[Title Page](#)[Abstract](#)[Introduction](#)[Conclusions](#)[References](#)[Tables](#)[Figures](#)[◀](#)[▶](#)[◀](#)[▶](#)[Back](#)[Close](#)[Full Screen / Esc](#)[Printer-friendly Version](#)[Interactive Discussion](#)

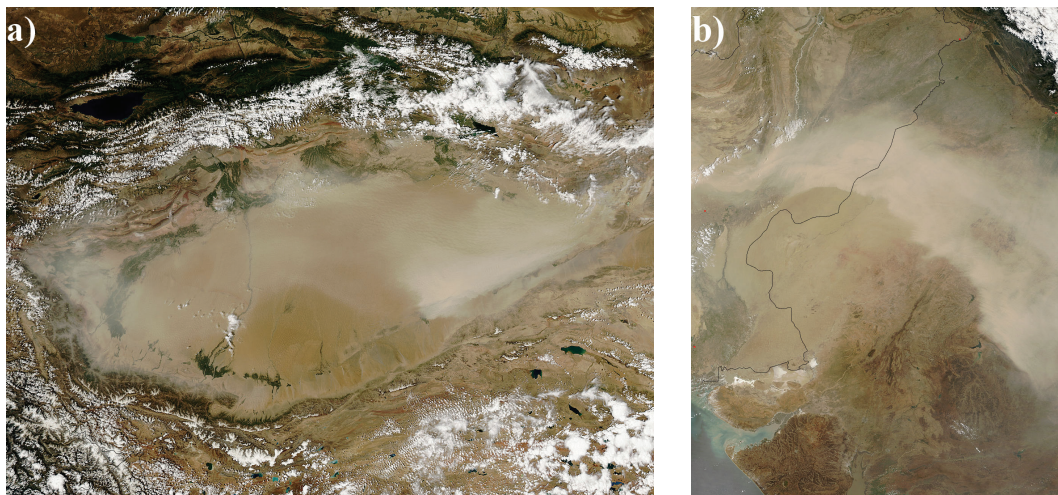
Spatial variability of aerosol, clouds and rainfall in HimalayasP. Shrestha and
A. P. Barros

Fig. 5. MODIS image of dust storm over Taklamaman Desert, northern slopes of Tibetan Plateau **(a)** and Thar Desert, north-western part of India **(b)**, source: VISIBLE EARTH NASA Image.

[Title Page](#)[Abstract](#)[Introduction](#)[Conclusions](#)[References](#)[Tables](#)[Figures](#)[⏪](#)[⏩](#)[◀](#)[▶](#)[Back](#)[Close](#)[Full Screen / Esc](#)[Printer-friendly Version](#)[Interactive Discussion](#)

Spatial variability of aerosol, clouds and rainfall in Himalayas

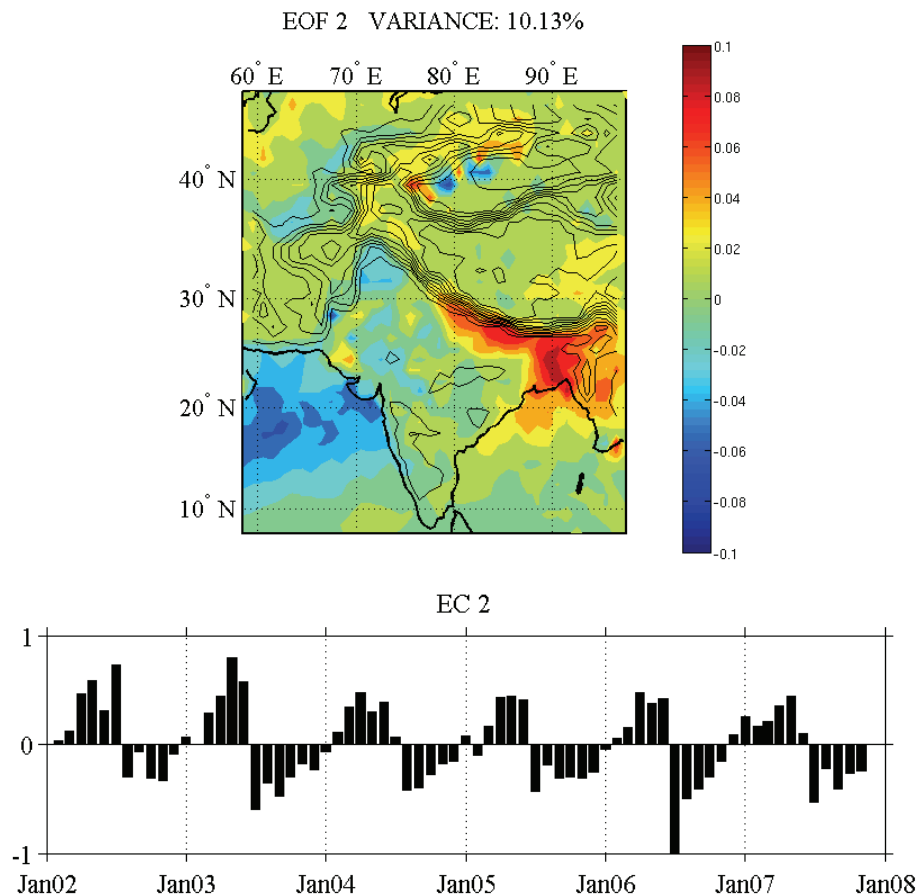
P. Shrestha and
A. P. Barros

Fig. 6. EOF 2 and EC2 computed from MODIS AOD product indicate a spatial mode on the southern slopes of Himalayas over Nepal bounded by the Arvalli range in the west and Bay of Bengal on the east.

[Title Page](#)[Abstract](#)[Introduction](#)[Conclusions](#)[References](#)[Tables](#)[Figures](#)[◀](#)[▶](#)[◀](#)[▶](#)[Back](#)[Close](#)[Full Screen / Esc](#)[Printer-friendly Version](#)[Interactive Discussion](#)

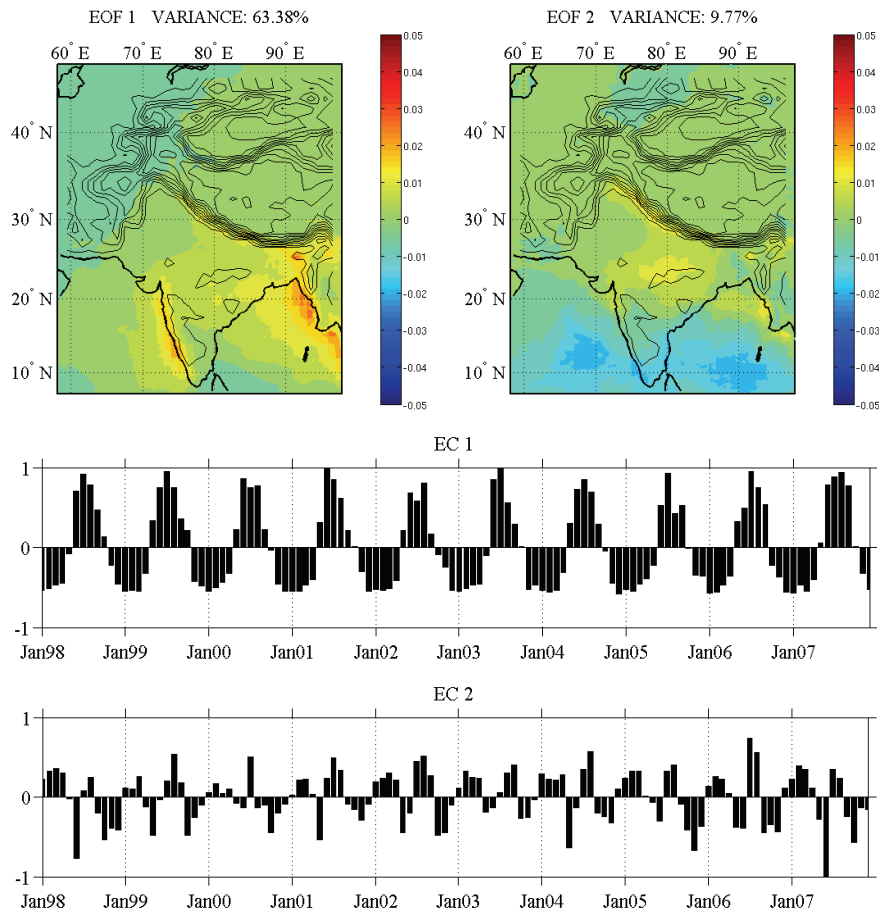
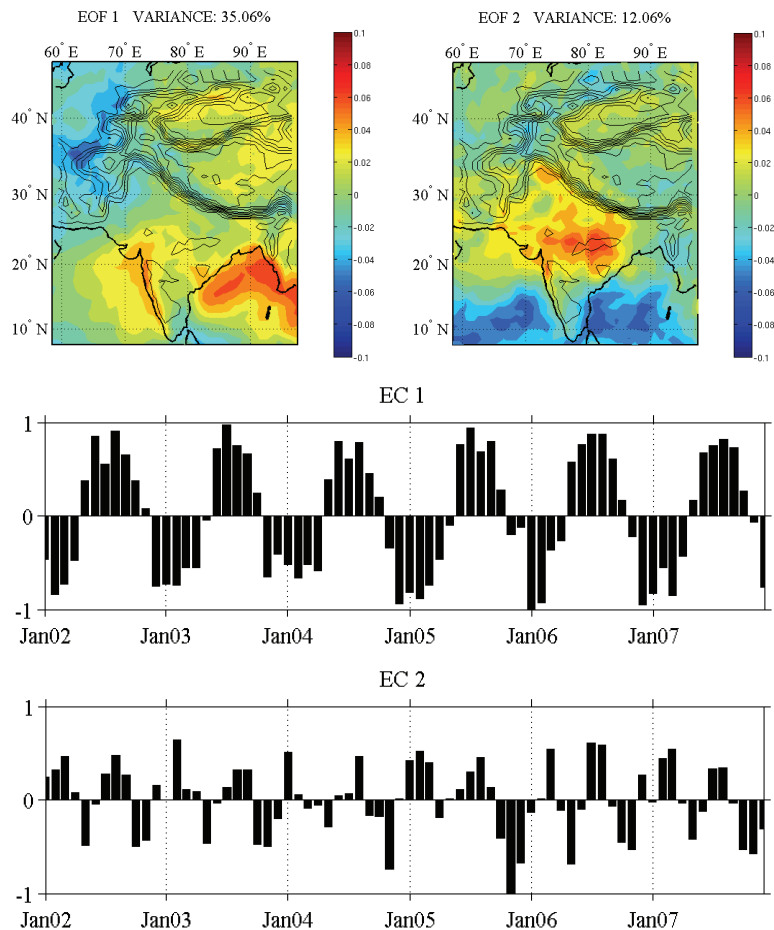
Spatial variability of
aerosol, clouds and
rainfall in HimalayasP. Shrestha and
A. P. Barros

Fig. 7. EOF 1, EC1 and EOF2, EC2 computed from TRMM monthly accumulated rainfall product.

[Title Page](#)[Abstract](#)[Introduction](#)[Conclusions](#)[References](#)[Tables](#)[Figures](#)[◀](#)[▶](#)[◀](#)[▶](#)[Back](#)[Close](#)[Full Screen / Esc](#)[Printer-friendly Version](#)[Interactive Discussion](#)

Spatial variability of aerosol, clouds and rainfall in HimalayasP. Shrestha and
A. P. Barros**Fig. 8.** EOF 1, EC1 and EOF2, EC2 computed from MODIS cloud optical depth (COD) product.[Title Page](#)[Abstract](#)[Introduction](#)[Conclusions](#)[References](#)[Tables](#)[Figures](#)[◀](#)[▶](#)[◀](#)[▶](#)[Back](#)[Close](#)[Full Screen / Esc](#)[Printer-friendly Version](#)[Interactive Discussion](#)

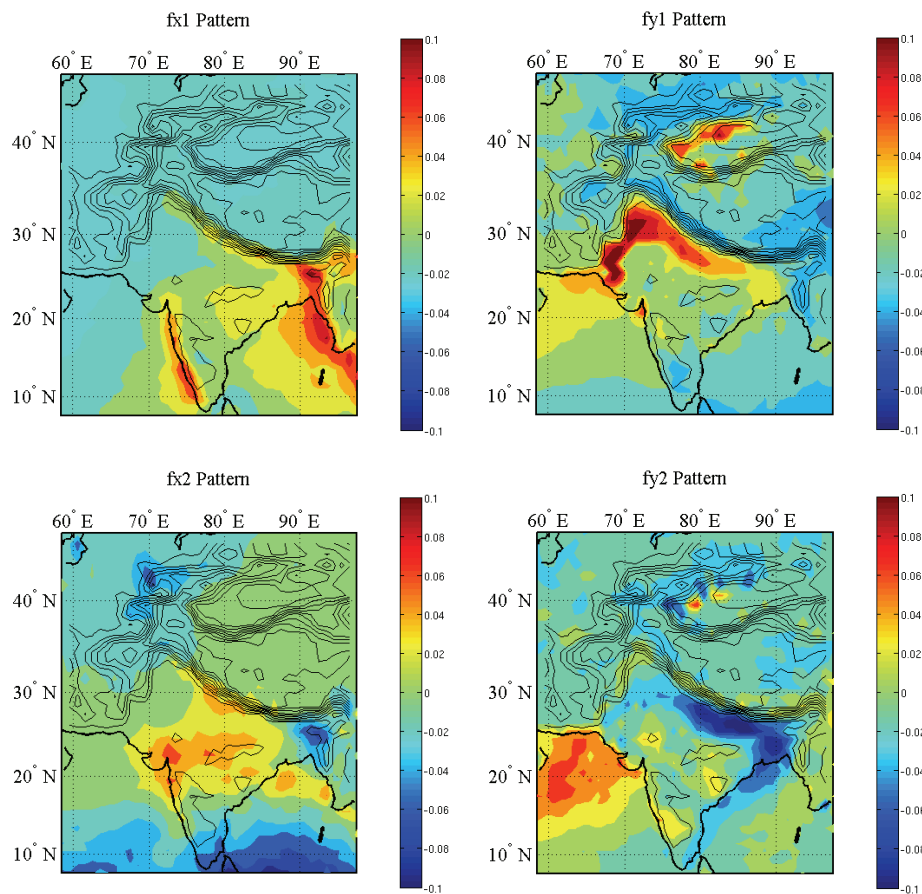
Spatial variability of
aerosol, clouds and
rainfall in HimalayasP. Shrestha and
A. P. Barros

Fig. 9. The first two spatial patterns of TRMM precipitation ($fx1, fx2$) and MODIS AOD ($fy1, fy2$) that explain the maximum covariance between the two fields.

[Title Page](#)[Abstract](#)[Introduction](#)[Conclusions](#)[References](#)[Tables](#)[Figures](#)[⏪](#)[⏩](#)[◀](#)[▶](#)[Back](#)[Close](#)[Full Screen / Esc](#)[Printer-friendly Version](#)[Interactive Discussion](#)

Spatial variability of aerosol, clouds and rainfall in Himalayas

P. Shrestha and
A. P. Barros

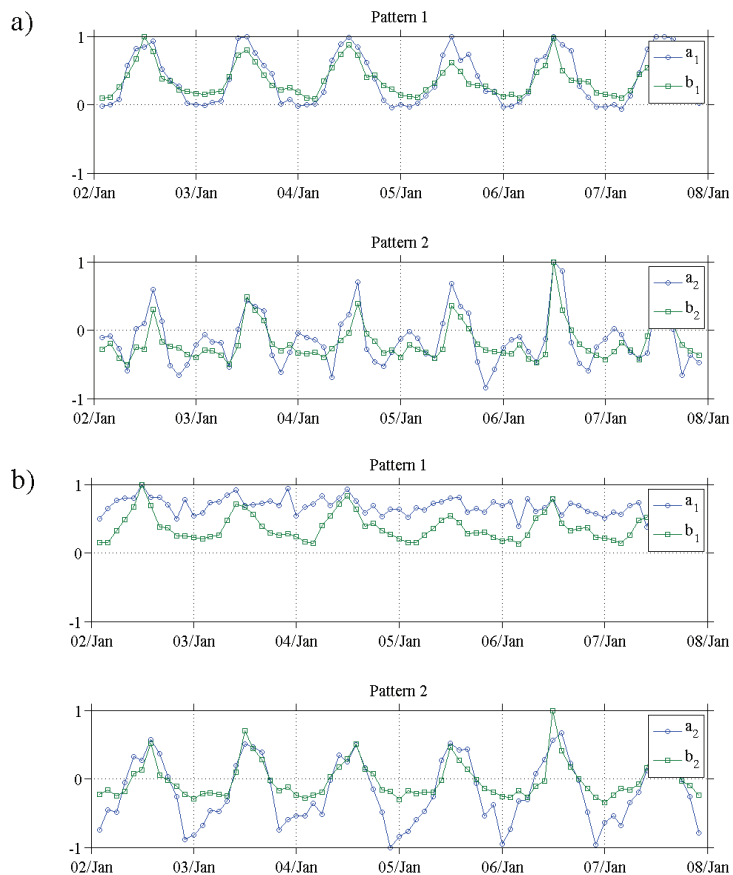


Fig. 10. The time series of the expansion coefficients between the pair of patterns: **(a)** Spatial patterns of TRMM precipitation and MODIS AOD, **(b)** spatial patterns of MODIS COD and MODIS AOD.

[Title Page](#)
[Abstract](#)
[Introduction](#)
[Conclusions](#)
[References](#)
[Tables](#)
[Figures](#)
[◀](#)
[▶](#)
[◀](#)
[▶](#)
[Back](#)
[Close](#)
[Full Screen / Esc](#)
[Printer-friendly Version](#)
[Interactive Discussion](#)

Spatial variability of aerosol, clouds and rainfall in Himalayas

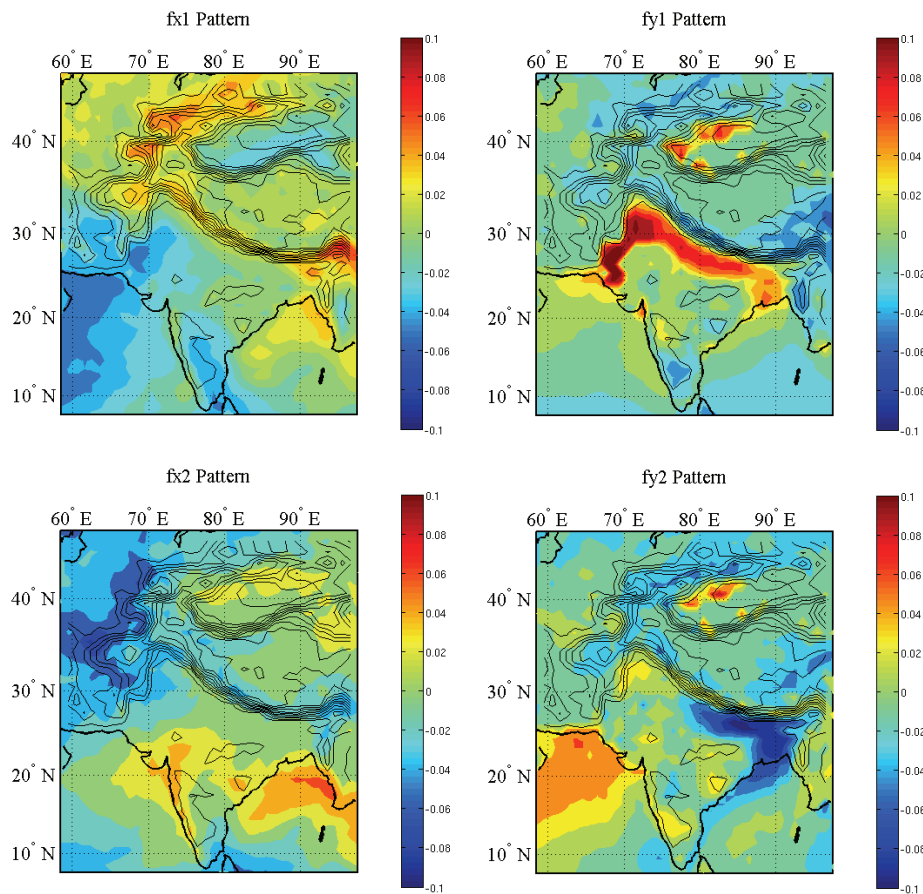
P. Shrestha and
A. P. Barros

Fig. 11. The first two spatial patterns of MODIS COD (f_{x1}, f_{x2}) and MODIS AOD (f_{y1}, f_{y2}) that explains the maximum covariance between the two fields.

[Title Page](#)[Abstract](#)[Introduction](#)[Conclusions](#)[References](#)[Tables](#)[Figures](#)[◀](#)[▶](#)[◀](#)[▶](#)[Back](#)[Close](#)[Full Screen / Esc](#)[Printer-friendly Version](#)[Interactive Discussion](#)

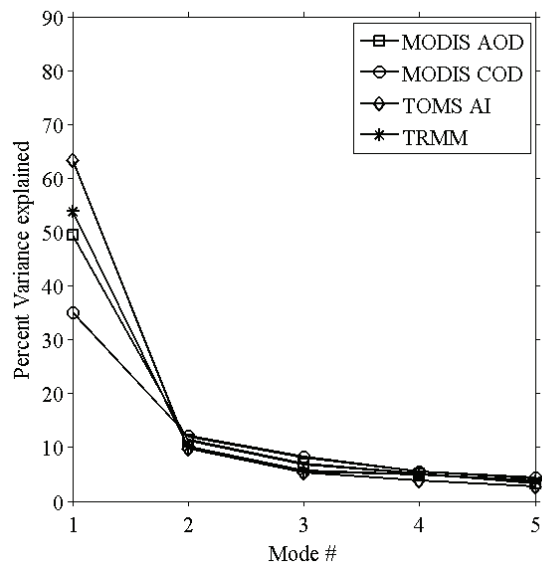
Spatial variability of aerosol, clouds and rainfall in HimalayasP. Shrestha and
A. P. Barros

Fig. 12. Distribution of the relative contribution of the first 5 modes to the overall spatial variance for MODIS AOD, MODIS COD, TOMS AI and TRMM precipitation.

[Title Page](#)[Abstract](#)[Introduction](#)[Conclusions](#)[References](#)[Tables](#)[Figures](#)[◀](#)[▶](#)[◀](#)[▶](#)[Back](#)[Close](#)[Full Screen / Esc](#)[Printer-friendly Version](#)[Interactive Discussion](#)